Time Domain Classification and Quantification of Seismic Noise

Jörn Groos[1], Joachim R. R. Ritter[1]

[1] Geophysikalisches Institut, Universität Karlsruhe (TH), Germany, E-mail: joern.groos@gpi.uni-karlsruhe.de, joachim.ritter@gpi.uni-karlsruhe.de

Introduction

Currently several efforts are undertaken in seismology to retrieve information about the underground from ambient seismic noise (e.g. Curtis et al. 2006; Shapiro et al. 2005; Sens-Schönfelder & Wegler 2006).
Such studies are especially interesting in areas where traditional seismic methods are complicated such as remote areas with poor access and cities. E.g. a large number of passive seismic measurements in urban environments are undertaken with the aim to provide the required underground information for seismic hazard assessment. Seismological research must significantly improve the understanding of (urban) seismic noise to successfully and reliably apply these new methods in urban environments (Bonnefoy-Claudet et al. 2006; Campillo 2006). A good knowledge of the seismic noise conditions and contributing noise sources are crucial to select adequate time windows of available long-term data or to design short-term measurements.

We present a statistical classification scheme in the time domain to quantify and characterise seismic noise. The character of seismic noise (e.g. Gaussian distributed or dominated by single signals) is represented by only six noise classes. This approach allows us to easily visualise the seismic noise properties (amplitude and statistical properties). Furthermore, it provides a reduced dataset from broadband seismic waveforms to analyse temporal and spatial changes of seismic noise conditions.

Dataset

The proposed classification scheme was developed to analyse the urban seismic noise (USN) dataset collected during the URban Seismology (URS) project (Ritter et al. 2005). The URS project was conducted in Bucharest (Figure 1), the capital of Romania, whose 2.5 million inhabitants are endangered by devastating earthquakes from the Vrancea subduction zone (for a comprehensive review see Wenzel et al. 1999). The measurements within the URS project were conducted with the KArlsruhe BroadBand Array (KABBA) owned by the Universität Karlsruhe (TH), Germany. The URS dataset was recorded with 32 24-bit dataloggers (EarthData) and 22 Streckeisen STS-2 (fundamental period T_0=120 s), five Geotech KS-2000 (T_0=100 s), two Güralp CMG40T (T_0=30 s), one Güralp CMG3ESP (T_0=30 s) and two Lennartz LE3D/5s (T_0=5 s) seismometers.
These stations were deployed at 34 different sites within the metropolitan area of Bucharest from October 2003 until August 2004 (Figure 1). The instruments were mainly located in cellars of public and private buildings.

Noise classification

Broadband (urban) seismic noise must be considered as a temporally and spatially non-stationary random process. This random process is generated by an unknown number of signals emitted by numerous independent and spatially distributed sources with unknown properties. Such a summation of an infinite large number of independent signals can be expected as Gaussian distributed as expressed by the central limit theorem.

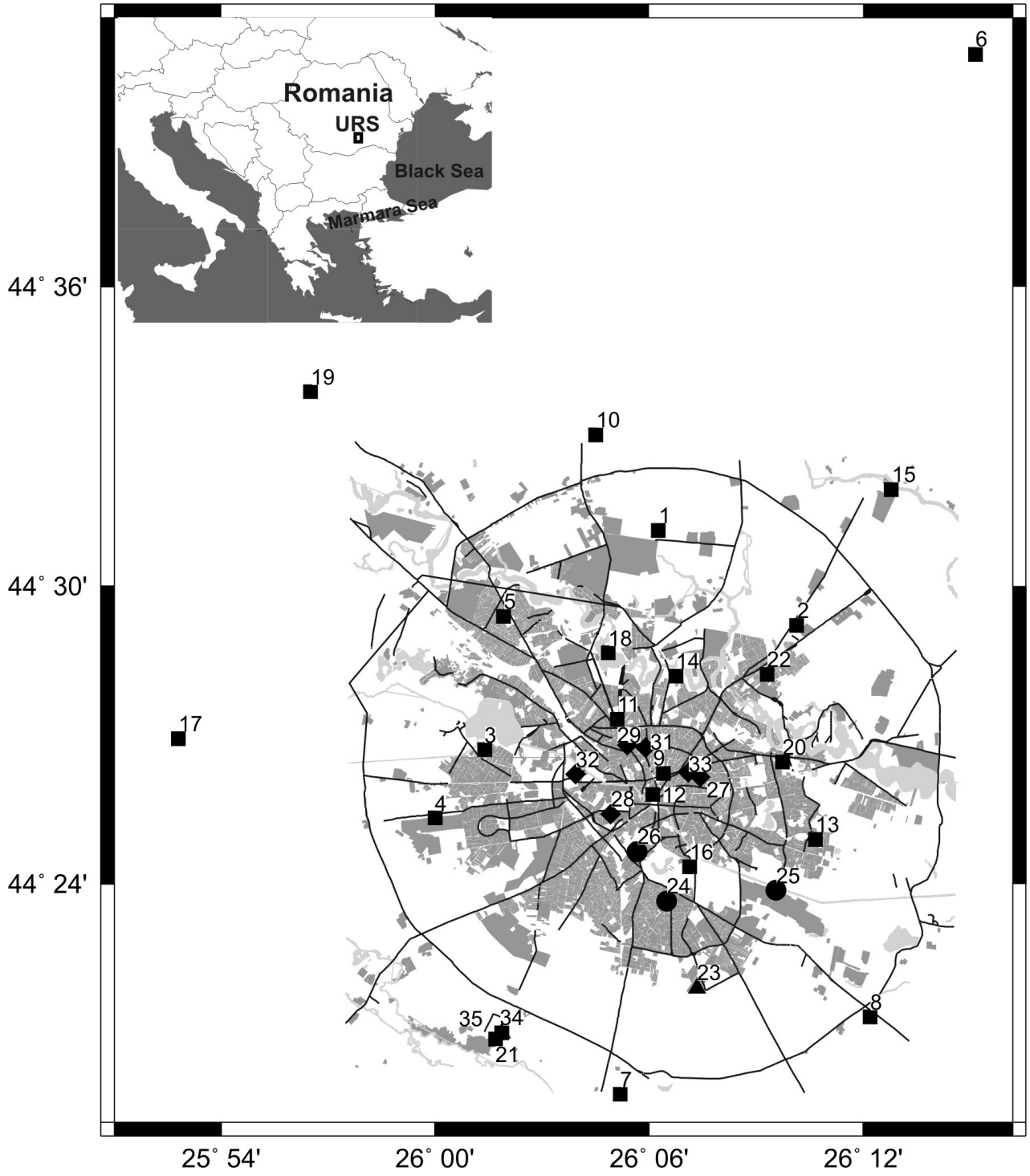

Figure 1: Station network of the URban Seismology (URS) project in Bucharest, Romania and its surroundings. Different symbols indicate different sensor types, squares: 22 Streckeisen STS-2, diamonds: 5 Geotech KS-2000, circles: 3 Güralp CMG40T and CMG3ESP, and triangles: 2 Lennartz LE3D/5s. The inset displays the regional context.

Nevertheless, finite time series of seismic noise may exhibit deviations from the Gaussian distribution due to the emergence of single or few dominating signals above the background signal. By analysing 4 hours long time windows of urban seismic noise in Bucharest, we observed several common deviations of their histograms (sample value distributions of the time series) from the Gaussian distribution. Most common deviation from the Gaussian distribution is a positive kurtosis of the histogram due to the presence of transient signals with short duration (seconds to minutes) and large amplitudes in comparison to the background signal (Figure 2c+d). Less common are bell-

shaped or multi-modal histograms with a negative kurtosis (Figure 2e). These deviations are most commonly caused by the dominance of long-lasting periodic signals. In rare cases we observed time series with asymmetric histograms due to the presence of asymmetric signals (Figure 2f).

We utilise ratios of amplitude intervals (I) and percentiles (P) to identify and quantify the deviations of the time series histogram from the Gaussian distribution. In the case of a zero mean Gaussian distribution, 68% of the measurements lie within an interval of one standard deviation away from zero (I68). 95.45% are within two times the standard deviation (I95) and 99.73% are within three times the standard deviation (I99). This is also known as the 2-σ and 3-σ, or the 'empirical', rule. Furthermore, the ratios of the lower and upper boundaries of the intervals (e.g. the 16-percentile (P16) and the 84-percentile (P84) for I68) can reveal a possible skewness of the histogram and can be used as a symmetry measure.

The intervals I95 and I99 are indicated by solid (I95) and dash-dot (I99) lines at the corresponding percentiles in Figure 2. The ratios between the intervals (I68, I95 and I99) and the corresponding percentiles of the time series are used to classify the seismic noise time series. Basic idea is that the interval ratios increase in the case of a positive kurtosis and decrease in the case of a negative kurtosis of the histogram. We introduce the ratio between I99 and I95 as the quantity peakfactor (pf) to determine the kurtosis of the histogram. The peakfactor of a Gaussian distributed time series equals 1.5. The range of the 68%-interval is used for quantification and called 'noise amplitude'.

We introduce six noise classes to classify the typically observed deviations from the Gaussian distribution (Figure 2). Time series are assumed to be Gaussian distributed if the interval ratios exhibit only very small deviations from the empirical rule and the histograms are symmetric (see Table 1). Gaussian distributed time series are classified as noise class 1 (NC1, Figure 2a).

Noise class	I95/ I68	I99/ I68	P84/ |P16|	P97.5/ |P2.5|
1	2±0.05	3±0.15	1±0.015	1±0.015

Table 1: Criteria for the interval and percentile ratios to classify a time series as Gaussian distributed (NC1).

Non-Gaussian symmetric time series (see Table 2) are classified as NC2-NC5 depending on the observed deviation properties. Time series which exhibit determinable but rather small and unspecific deviations from the Gaussian distribution (pf 1.5±0.1) are classified as noise class 2 (Table 2 and Figure 2b). Time series with a gentle positive kurtosis ($1.6<pf\leq2$) due to few transient signals are classified as noise class 3 (Figure 2c). A more pronounced positive kurtosis of the histogram ($pf>2$) results in a classification of the time series as noise class 4 (Figure 2d). Symmetric time series with a negative kurtosis ($pf<1.4$) are classified as noise class 5 (Figure 2e).

NC	peakfactor	P84/|P16|	P97.5/|P2.5|
2	1.5±0.1	1±0.03	1±0.047
3	$1.6<pf\leq2.0$	1±0.03	1±0.047
4	$2.0<pf$	1±0.03	1±0.047
5	$pf<1.4$	1±0.03	1±0.047

Table 2: Criteria for the interval and percentile ratios to classify symmetric time series as noise classes NC2-NC5.

All time series which are not identified as symmetric time series (see Table 2) are classified as noise class 6.

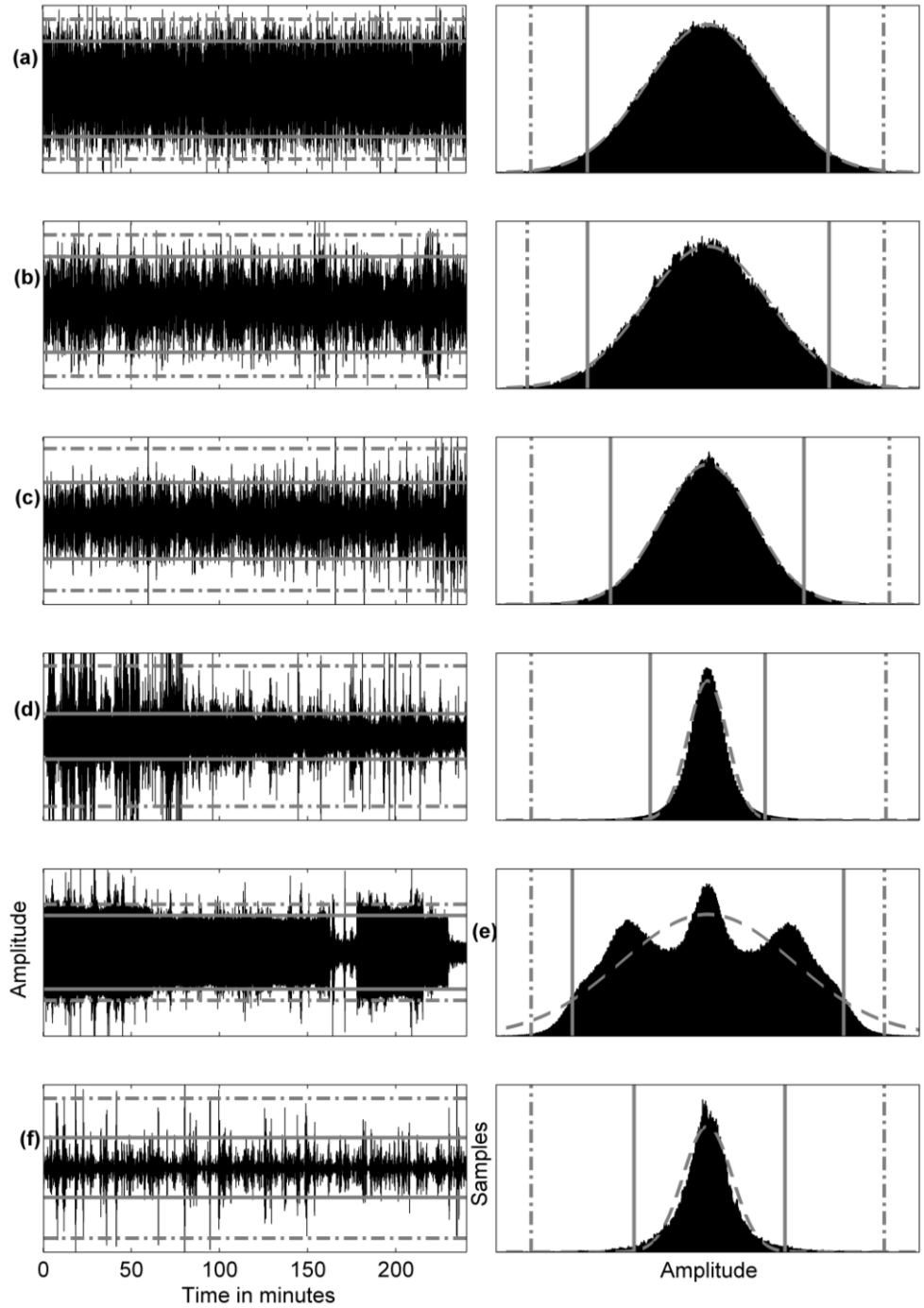

Figure 2: Time series (left) of vertical component urban seismic noise (USN) recorded in Bucharest and their histograms (distribution of sample values) (right) together with the Gaussian distributions (dashed lines) estimated from the mean and the upper boundary of the 68%-interval of the corresponding time series. The 95.45- (solid lines) and 99.73- (dash-dot lines) intervals are indicated, corresponding to the 2-σ and 3-σ range respectively for a Gaussian distributed time series. (a) Gaussian distributed time series of the USN(0.25-0.6 Hz) at site URS02 with a peakfactor of 1.47. (b) Nearly Gaussian distributed time series (NC2) of the USN(0.04-0.09 Hz) at site URS06 with a peakfactor of 1.48. The minor deviations from the Gaussian distribution are small and caused by short transient events with double-amplitudes larger than the range of the 99.73%-interval (left panel). (c) Time series of the USN(0.18-0.25 Hz) at site URS04 dominated by short transient noise signals (NC3) resulting in a peakfactor of 1.85. The histogram is slightly deformed at the tails in comparison to the estimated Gaussian distribution. (d) Time series of the USN(1-25 Hz) at site URS01 dominated by short transient noise signals (NC4) resulting in a peakfactor of 3.1. The histogram is heavily deformed at the tails in comparison to the estimated Gaussian distribution. (e) Time series of the USN(1-25 Hz) at site URS20 with a peakfactor of 1.3 and a non bell shaped multi-modal distribution (NC5). The displayed time series is dominated by sinusoidal signals. (f) Time series of the USN(0.04-0.09 Hz) at site URS26 with an asymmetric distribution (NC6) due to the dominance of asymmetric signals.

Noise analysis

We calculated long-term spectrograms of up to 28 days duration to identify the frequency-dependent behaviour of the time-variable seismic noise in Bucharest. We selected several frequency ranges between 8 mHz and 45 Hz for the time domain classification to capture the frequency-dependent variability of seismic noise. Furthermore we selected 3 time windows with 4 hours duration (0-4, 8-12 and 13-17 local time) for the noise classification to capture the temporal variability of the urban seismic noise with daytime. The results of the time domain classification for the urban seismic noise in Bucharest are given in four frequency ranges (Table 3). These frequency ranges are dominated by ocean-generated microseism (0.09-0.18 Hz), wind (0.6-1 Hz) and human activity (0.6-45 Hz).

Frequency/Hz	Dominating noise sources
0.09-0.18	secondary ocean-generated microseism
0.6-1	wind, human activity
1-25	human activity
25-45	human activity

Table 3: Frequency ranges for the statistical time-series analysis. Depending on the frequency range different noise sources dominate the urban seismic noise in Bucharest.

The noise conditions in terms of noise amplitudes and noise classes are visualised for the 4 hours long time windows at day and night by noise maps of the metropolitan area of Bucharest (Figure 3). The range of the 68%-interval is given as noise amplitude by colour and the noise classification is given as symbol at the station site. The noise amplitudes are interpolated between station sites for visualisation. These maps are tools to analyse large amounts of output data and are not intended to estimate noise amplitudes between station sites.

The influence of human activity can be observed by statistical properties which systematically vary with daytime in the frequency ranges between 0.09 and 45 Hz. The temporal varying amount of transient and periodic man-made signals contributing to the urban seismic noise (USN) significantly influences the histograms of the analysed time windows.

In the frequency range 0.09-0.18 Hz natural sources of seismic energy, especially secondary ocean-generated microseism, dominate the USN in Bucharest. Due to the larger amplitudes of these naturally induced seismic waves the influence of human activity is not as obvious as at higher frequencies larger than 1 Hz as found from the variation of noise amplitudes between day and night. Nevertheless, the influence of human activity can be observed by changes of the statistical properties with daytime. The amount of time series with significant deviations from the Gaussian distribution (NC3-NC6) increases from less than 20% at night to more than 40% at day. Besides the temporal variability of USN(0.09-0.18 Hz) noise amplitudes in correlation with the ocean-generated microseism, we observe a systematic spatial variation of noise amplitudes. The noise amplitudes increase from the southern part of the metropolitan area towards north. The same spatial effect of ground motion amplification was observed by two amplitude and site effect studies utilising earthquake signals and is explained with resonance effects in the unconsolidated sediments above the dipping Neogene-Cretaceous boundary (Sudhaus & Ritter 2009; Mandrescu et al. 2004). Our similar observation for the noise amplitudes demonstrates the potential of noise amplitude mapping to complement information for site effect studies.

In the frequency range 0.6-1 Hz urban seismic noise in Bucharest is dominated by man-made ground motion as long as the wind velocity is below 3 m/s (Figure 3). The spatial variation of noise amplitude is in well correlation with the varying density of population indicated by an increase of noise amplitudes towards the city centre (Figure 3). Uncommonly large noise amplitudes are observed in vicinity (<500 m) to a heavy industry area in the south-eastern part of Bucharest (Figure 3). The large amount of man-made transient signals during the day results in Gaussian distributed seismic noise at most station sites. At night the remaining transient signals cause significant deviations from the Gaussian

distribution (Figure 3). With wind velocities exceeding 3 m/s the USN is increasingly dominated by wind-induced ground motion. This change of the dominating noise source is accompanied by significant changes of the spatial noise amplitude distribution and the statistical properties.

In the frequency range 1-45 Hz man-made transient signals characterise the USN in Bucharest at day and night. The noise amplitudes in the frequency ranges 1-25 Hz and 25-45 Hz increase towards the city centre at day and night. Inside the inner city area we observe a heterogeneous spatial distribution of the highest noise amplitudes. The amplitude increase corresponds in principle very well with the increasing population density towards the city centre. However, at some sites distinct higher amplitudes are observed. Except the city centre sites all sites with high noise amplitudes are in vicinity (<500 m) of busy heavy industry areas.

Outlook

Our classification scheme is able to discriminate different seismic noise situations on a quantitative basis. It works well in a complicated area such as a lively city with numerous noise sources. Further studies are under way to apply this method to other seismological and technical situations.

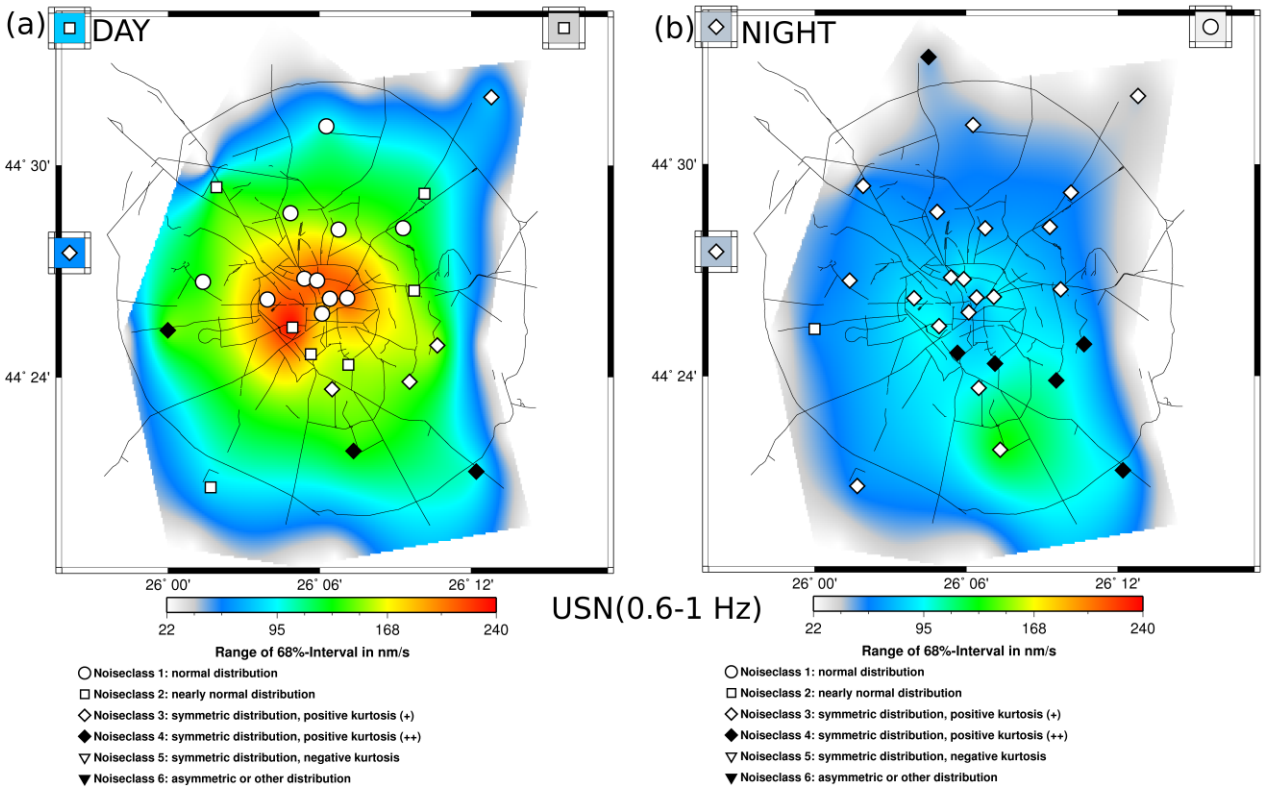

Figure 3: Maps of Bucharest with average urban seismic noise amplitudes and noise classification at station sites (symbols). Displayed are the noise amplitudes (range of the 68%-interval) of the ground motion velocity in nm/s in the frequency range 0.6-1 Hz on 2004-Feb-03. (a) daytime (13-17pm EET). (b) nighttime (00-04am EET). Stations URS06, URS17 and URS19 (outside the city area, see Figure 1) are displayed in separate boxes at the edges. Surface gridding was done by GMT (www.gmt.soest.hawaii.edu) with the continuous curvature surface gridding algorithm (Smith & Wessel 1990) under a tension of 0.1. This interpolation preserves measured amplitude values at the station sites. The lower limit of the interpolation output is 90 percent of the smallest measured noise amplitude. The upper limit is the largest measured noise amplitude. Between station sites interpolation effects may occur due to partly large inter-station differences in amplitude. Real noise amplitudes cannot be derived between station sites. These maps are mainly visualisation tools to analyse large amounts of output data and search for temporal and spatial variations.

References

Bonnefoy-Claudet, S., F. Cotton and P-Y. Bard, The nature of noise wavefield and its application for site effects studies – a literature review, Earth Sc. Rev., 79, 205-227, doi:10.1016/j.earscrev.2006.07.004, 2006.

Campillo, M., Phase and Correlation in Random Seismic Fields and the Reconstruction of the Green Function, Pure and Applied Geophysics, 163, 475–502, 2006.

Curtis, A., P. Gerstoft, H. Sato, R. Snieder and K. Wapenaar, Seismic interferometry – turning noise into signal, The Leading Edge, 25, 1082-1092, 2006.

Mandrescu N., M. Radulian and G. Marmureanu, Site conditions and predominant period on seismic motion in the Bucharest urban area, Revue Roumaine de Geophysique, 48, 37-48, 2004.

Ritter, J. R. R., S. F. Balan, K.-P. Bonjer, T. Diehl, T. Forbriger, G. Marmureanu, F. Wenzel and W. Wirth, Broadband Urban Seismology in the Bucharest Metropolitan Area, Seismological Research Letters, 76, 574–580, 2005.

Sens-Schönfelder, C. and U. Wegler, Passive image interferometry and seasonal variations of seismic velocities at Merapi volcano, Indonesia, Geophys. Res. Lett., 33, L21302, doi:10.1029/2006GL027797, 2006.

Shapiro, N. M., M. Campillo, L. Stehly and M. H. Ritzwoller, High-resolution surface-wave tomography from ambient seismic noise, Science, 307, 1615-1618, 2005.

Smith, W. H. F. and P. Wessel, Gridding with continuous curvature splines in tension, Geophysics, 55, 293-305, 1990.

Sudhaus, H. and J. R. R. Ritter, Broadband frequency-dependent amplification of seismic waves across Bucharest, Romania, Journal of Seismology, DOI 10.1007/s10950-008-9140-0, 2009.

Wenzel, F., D. Lungu and O. Novak, *Vrancea earthquakes tectonics, hazard and risk mitigation*, Kluwer Academic Publishers, Dordrecht, Boston, 1999.